Materials Today: Proceedings xxx (xxxx) xxx

Contents lists available at ScienceDirect

Materials Today: Proceedings

journal homepage: www.elsevier.com/locate/matpr

Multicomponent Sn–Mo–O-containing films formed in anodic alumina matrixes by ionic layer deposition

Anna Zakhlebayeva *, Andrei Lazavenka, Gennady Gorokh

R&D Laboratory Nanotechnologies, Belarusian State University of Informatics and Radio Electronics, P. Brovki St. 6, 220013 Minsk, Belarus

ARTICLE INFO

Article history:
Received 31 July 2019
Received in revised form 13 July 2020
Accepted 8 September 2020
Available online xxxx

Keywords:
Successive ionic layer adsorption and reaction (SILAR)
Porous anodic alumina
Structured surface
Tin-molybdenum oxide
Multicomponent metaloxides
Structure characterization

ABSTRACT

Multicomponent metal oxide compounds of the composition Sn–Mo–O, Sn–Ni–Mo–O and Sn–Bi–Mo–O were formed by successive ionic layer adsorption and reaction (SILAR) method deposition into anodic alumina matrixes. The growth mechanism of the Sn–Mo–O-containing films in the porous anodic alumina was investigated. It was found that the degree of pore filling, specific thickness and surface morphology of the deposited layer depend not only on the number of cycle's treatment, but also on the composition of the used solutions. The morphology of Sn–Mo–O and Sn–Ni–Mo–O surfaces had granular structures, while Sn–Bi–Mo–O layer had flake-like structure. The differences in microstructure and deposition of the layers on the surface of the matrixes can be explained by the insufficient activation of anodic alumina pores before deposition. The investigations of the formed layers composition by the electron-probe X-ray spectral microanalysis showed that the ratio of tin to molybdenum in tin-molybdenum containing oxides changes. The Sn/Mo atomic ratio for Sn–Mo–O layer is 1.29/2.72; for Sn–Ni–Mo–O layer is 5.83/4.85; for Sn–Bi–Mo–O layer is 0.60/0.87. The using of SILAR method allows forming multicomponent films in the anodic alumina matrixes, which have great potential to applicate in high-sensitivity gas sensors.

Selection and peer-review under responsibility of the scientific committee of the International Conferences & Exhibition on Nanotechnologies, Organic Electronics & Nanomedicine.

1. Introduction

The successive ionic layer deposition method, well known as successive ionic layer adsorption and reaction (SILAR), is one of the most promising chemical methods of thin films formation with various compositions. The SILAR method is based on cycle treatment of substrates in ion-containing solutions such as metal chlorides, nitrates, and acetates. As a result of reaction between adsorbed metal cations and anions, a nanolayer of hard-to-dissolve compound is formed on the substrate surface [1]. At the present time, the SILAR method is widely used for metal chalcogenides and metal oxides formation to following application in solar cells and gas sensors respectively [2–5]. Also, some discoveries of metal phosphates formation by the SILAR method are known [6], but nowadays this method is not very common for producing of such type compounds.

The metaloxide thin films have great-applied significance as sensitive layers for chemoresistive gas sensors. Such type of sensors still is the largest and the most investigated group of sensing devices; lots of researches are forward to improve sensor's characteristics, such as sensitivity, selectivity, response time, etc. [7–10]. On the whole, mechanism of metaloxides chemoresistivity can be explained by redox reactions in the metaloxide layer [7–10]. During exposure to the air, oxygen ions are being adsorbed on the metaloxide layer surface which leads to change surface charge [11]. The adsorbed ions stand as traps for the electrons, so capture of the electrons from the metaloxide results in changes the space charge in the near-surface semiconductor area [11]. Depending on gas type (reduction or oxidation) and type of the metaloxide layer's conductivity (n- or p-), the reaction between gas molecules and surface oxygen could lead to return or far more capture of the electrons from the layer bulk which result in increasing or decreasing of the sensitive metaloxide layer conductivity [7–11]. At the present, the most using materials are oxides of Sn, Mo, W, Mn, Ni, Bi, In, Cu, which chemoresistive properties are well researched. One of the most common problems is poor selectivity of such

* Corresponding author.
E-mail address: zakhlebayeva@bsuir.by (A. Zakhlebayeva).

https://doi.org/10.1016/j.matpr.2020.09.252
2214-7853/
Selection and peer-review under responsibility of the scientific committee of the International Conferences & Exhibition on Nanotechnologies, Organic Electronics & Nanomedicine.

oxides, so it is suggested that using of the multicomponent metaloxides, which include a few metals, would improve sensors characteristics. For this reason, a lot of works focus on formation of binary and complex metaloxides such as SnO_2–WO_3 [11], SnO_2–ZnO [12], SnO_2–NiO [13], Fe_2O_3–ZnO [14], Bi_2WO_6 [15], $Bi_2Sn_2O_7$ [16], etc.

The SILAR method is very attractive for the multicomponent metaloxides formation due to ability combining varieties of cation- and anion-containing solutions in one technological process. So, multicomponent layers having various compositions can be synthesised. It is known several mechanisms of the multicomponent metaloxides formation such as oxidation of the adsorbed metal cations by peroxianions (as La^{3+} or Ce^{3+} and NbO^{3-} during the formation of $La_xNbO_y{\cdot}nH_2O$ or $Ce_xNbO_y{\cdot}nH_2O$ compounds) or the reduction of heteropoly oximetalates (for example, the reduction of $H_7PW_{12}O_{42}$ by $SnCl_2$ solution) [4]. However, the most typical mechanism of the semiconductor multicomponent metaloxides formation is the reduction of the adsorbed anions by cations, as in the case of tin-molybdenum oxide synthesis [4,17]. First, cations Sn^{4+} are adsorbed on the substrate surface from $SnCl_2$ solution, and then anions MoO_2^{4-}, which are adsorbed from $(NH_4)_2MoO_4$ solution, are reducted by Sn^{4+}. As a result, hard-to-dissolve Sn_x-$MoO_y{\cdot}nH_2O$ compound is being formed [17].

At the present time, the mechanisms of thin films formation by the SILAR method on non-structured substrates, such as silicon, quartz, ITO-glass, have been well researched [4,17,18]. Although, there are almost no researches into layering of thin films on the structured substrates, in particular on the porous anodic alumina. The porous anodic alumina consists of oxide cells having self-organized hexagonal honeycomb-like structure; in the centre of each cell the pore is placed [19,20]. Diameters of the pores and of the oxide cells can be variable in wide ranges (from 10 to 400 nm for pores and from 50 to 600 nm for oxide cells) by choosing of anodization mode [21]. Due to self-organized and variable structure, the porous anodic alumina has been actively exploited as template for synthesis of various nanostructured materials such as nanodots [22], nanowires [23], nanotubes [24], nanocolumns [25], and nanolayers [26].

Deposition of the metaloxide compounds in anodic alumina matrixes (AAMs) allows to form nanostructured films having large active surface area [26,27]. Also, due to using of the SILAR method for the films deposition, it is possible to form layers having various compositions. Combination of the SILAR method with AAMs allows creating the systems which properties depend on their morphology and composition. So, investigations of the metaloxide films formation in the porous anodic alumina by the SILAR method are especially interesting nowadays.

This work presents the results of the Sn–, Mo–, Ni–, Bi–, O-containing films deposition in anodic alumina matrixes by the SILAR method and the morphological properties and elemental composition of formed structures.

2. Experimental details

2.1. Preparation of anodic alumina matrixes

Nanoporous AAMs were prepared by the two-step anodization of 1.2–1.4 μm aluminum films magnetron-sputtered on silicon substrates. Anodization process was performed in the aqueous solution of 0.2 mol·dm^{-3} tartaric acid. On the first step the aluminum film was anodized in the galvanostatic mode at current density of 6 mA cm^{-2} during 6.5 min. Formed anodic alumina was selective dissolved in $H_3PO_4 + CrO_3$ aqueous solution at T = 80 °C. This operation resulted in structuring of the aluminum surface by the oxide cells imprints. On the second step structured aluminum film was anodized in the potentiostatic mode at anodic potential of 210 V. The second anodizing step was performed until full oxidation of the aluminum film. Formed AAMs were treatment in $H_3PO_4 + CrO_3$ aqueous solution at T = 60 °C during 10.5 min to remove of anodic alumina layer containing acid anions and to widen the anodic alumina pores. By the two-step anodization method AAMs having thickness from 800 to 1000 nm and pore diameters from 250 to 320 nm were formed. Schematic process of the AAMs formation is shown in Fig. 1.

2.2. Formation of multicomponent metaloxide films in AAMs

The SILAR method is based on cycle treatment of AAM in cationic and anionic solutions, at that the matrix is rinsed in distilled water before every treatment to remove the loosely bounded ions and the reaction products. The surface of the AAM should be activated before treatment, i.e. on the matrix should be created the activation centers which cations can be adsorbed on. In general, one SILAR cycle involves the following steps:

(0) activation of the AAM surface;

(I) treatment of AAM in the cationic solution for cations adsorption on the matrix surface;

(II) rinsing of AAM in the distilled water for removal of cations loosely bound to surface;

(III) treatment of AAM in the anionic solution for anions adsorption, reduction of the adsorbed anions by cations, and a hard-to-dissolve compound layer formation;

(IV) rinsing of AAM in the distilled water for removal of reagents excesses and the reaction products.

Schematic mechanism of successive ionic layer deposition of the multicomponent metaloxide films in AAM is shown in Fig. 2.

In our case, AAMs were boiled in distilled water at T = 90–100 °C during 30 min to activate anodic alumina surface.

To deposit of Sn–Mo–O-containing films, tin (II) chloride was used as cationic solution and ammonium molybdate was used as anionic solution. One SILAR cycle involved the following steps:

(I) treatment of AAM in 0.1 mol·dm^{-3} $SnCl_2{\cdot}2H_2O$, pH = 1.35, T = 20 °C, t = 0.5 min;

(II) rinsing of AAM in H_2O (distilled), T = 20 °C, t = 1 min;

(III) treatment of AAM in 0.1 mol·dm^{-3} $(NH_4)_2MoO_4$, pH = 2.45, T = 20 °C, t = 0.5 min;

(IV) rinsing of AAM in H_2O (distilled), T = 20 °C, t = 1 min.

After one SILAR cycle, the Sn–Mo–O-containing monolayer was formed in AAM. Structures consisting of 10, 15, and 20 Sn–Mo–O-layers were formed and annealed in argon atmosphere at T = 750 °C during 30 min.

The layer deposition of Sn–Ni–Mo–O-containing films was performed according SILAR scheme. The compositions of 0.1 mol·dm^{-3} $SnCl_2{\cdot}2H_2O$ (pH = 1.35) and 0.1 mol·dm^{-3} $NiCl_2{\cdot}6H_2O$ (pH = 2.30) were used as cationic solutions, and 0.1 mol × dm^{-3} $(NH_4)_2MoO_4$ (pH = 2.45) was used as anionic solution. The modes of the AAM treatment (solutions temperature, time of treatment) were the same as for Sn–Mo–O-containing films deposition. During deposition of the Sn–Ni–Mo–O-containing compound, SILAR cycles interchanged in the following steps: (I) layering of Sn–Mo–O-containing compound; (II) layering of Sn–Mo–O-containing compound; (III) layering of Ni–Mo–O-containing compound. Thus, Ni–Mo–O-layer was being deposited after two Sn–Mo–O-layers. Generally, the formed film consists of 21 layers included 14 Sn–Mo–O- and 7 Ni–Mo–O-layers.

Also, deposition of Sn–Bi–Mo–O-containing films was performed according SILAR scheme by using cationic solutions 0.1 mol·dm^{-3} $SnCl_2{\cdot}2H_2O$ (pH = 1.35) and 0.1 mol·dm^{-3} $Bi(NO_3)_3{\cdot}5H_2O$ (pH = 0.19), and anionic solution 0.1 mol × dm^{-3} $(NH_4)_2MoO_4$ (pH = 2.45). Solutions temperature, time, and modes of the AAM treatment were the same as for Sn–Mo–O-containing

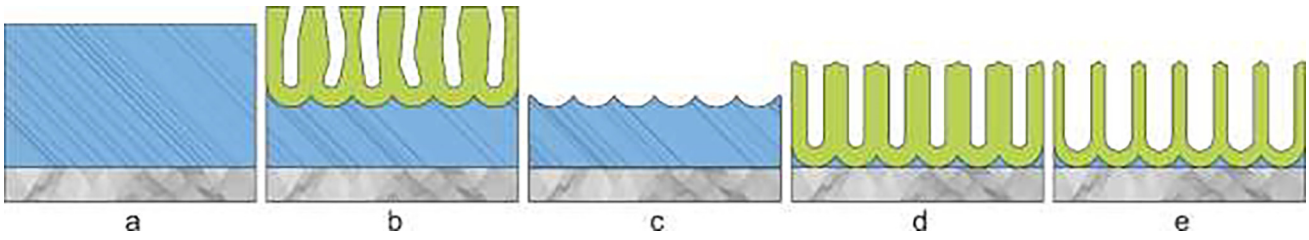

Fig. 1. Schematic process of AAMs formation: (a) magnetron-sputter of Al on Si substrate; (b) the 1st step of Al anodization; (c) selective removal of anodic alumina; (d) the 2nd step of Al anodization; (e) pore widening treatment of anodic alumina.

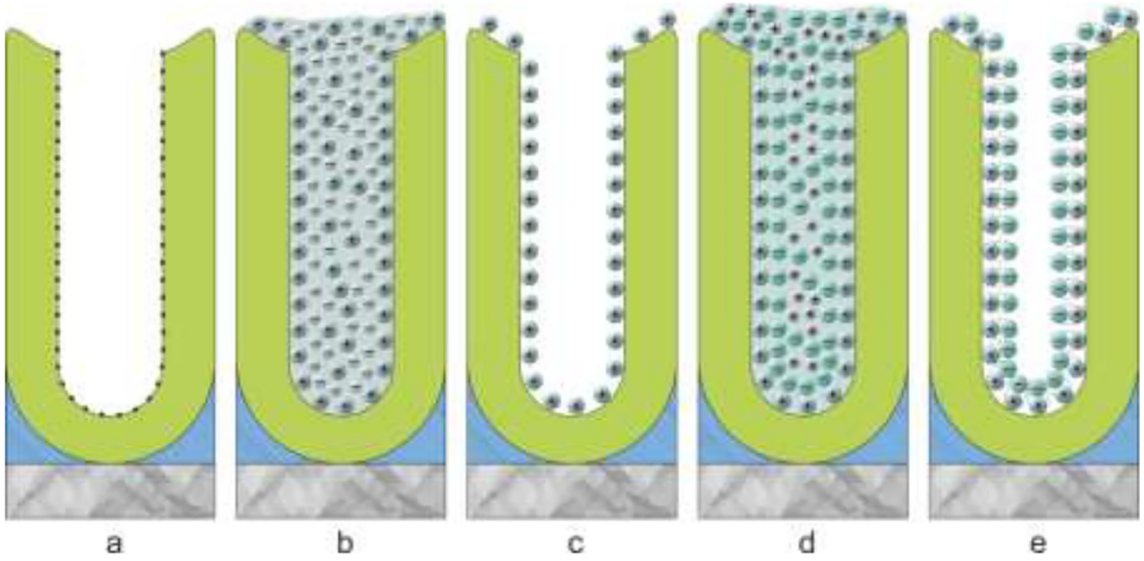

Fig. 2. Schematic mechanism of SILAR: (a) activation of AAM surface; (b) treatment of AAM in cationic solution; (c) rinsing of AAM (removal of cations loosely bound to surface); (d) treatment of AAM in anionic solution; (e) rinsing of AAM (removal of reagents excesses).

films deposition. During deposition, Bi–Mo–O-layer was formed after Sn–Mo–O-layer, i.e. SILAR cycles interchanged in the following manner: (I) layering of Sn–Mo–O-containing compound; (II) layering of Bi–Mo–O-containing compound. Formed film consists from 20 layers included 10 Sn–Mo–O- and 10 Ni–Mo–O-layers.

2.3. Films morphology and composition investigations

Morphology of the formed films were investigated by Scanning Electron Microscopy (SEM) method (scanning electron microscope "Hitachi S-806", accelerating voltage 10–15 kV, $(15–40) \times 10^3$ times magnification). Investigations of formed structures elemental compositions were performed by the electron-probe X-ray spectral microanalysis (EDX) using add-on "Bruker" for scanning electron microscope. Characteristic size of the spot from the primary ray was 2 μm. The penetration depth of the beam was from 0.1 to 2 μm.

Morphological parameters of formed structures (such as pores diameters, thicknesses of the films, grain sizes, etc.) were measured in the SEM images of surfaces and cross-sections by using the software ImageJ. Average values of morphological parameters were calculated based on measurement results.

3. Results and discussions

3.1. Morphology and composition of Sn–Mo–O-containing films

Morphology of the surfaces and the cross-sections of Sn–Mo–O-containing films formed in the AAM after 10, 15 and 20 SILAR cycles are shown in Fig. 3. It was observed, the formed films are layered along the pore walls and on the surface of anodic alumina. The film formed after 10 SILAR cycles is uniformly distributed over the porous surface of AAM, while the most part of the pores remained unfilled (Fig. 3a). After 15 cycles, the Sn–Mo–O-containing film was also uniformly distributed over the AAM surface. The thickness of the layer on the surface of the oxide cell walls was commensurate with the layer thickness at the bottom of the pores, but the entrances to the pores were still open (Fig. 3b). After 20 SILAR cycles, the AAM pores were almost completely filled, and the film thickness on the surface of the entire matrix was increased (Fig. 3c). The pore diameters of the initial AAM were decreased from 252 nm to 216, 128 and 80 nm after 10, 15 and 20 cycles, respectively.

Morphological parameters of formed Sn–Mo–O-containing films after 10, 15 and 20 SILAR cycles shown in Table 1.

Investigations of the morphological parameters have shown that the degree of pore filling with each subsequent cycle is not the identical. It was discovered, that the increasing in thickness after the first 10 cycles is noticeably greater than after the subsequent ones. So after 10 cycles the total layer thickness on the porous surface of the AAM was 111 nm, after 15 cycles – 125 nm, and after 20 cycles – 139 nm, that is, the thickness of the monolayer decreased with each cycle. This phenomenon can probably be explained by the transformation of the porous AAM microstructure during ion layering. Initially, a large number of activation centers were formed on the initial film, which cations were bound with. Then anions bound to them. Forming the first metal oxide layer. The deposition of each layer changed the morphology of the porous

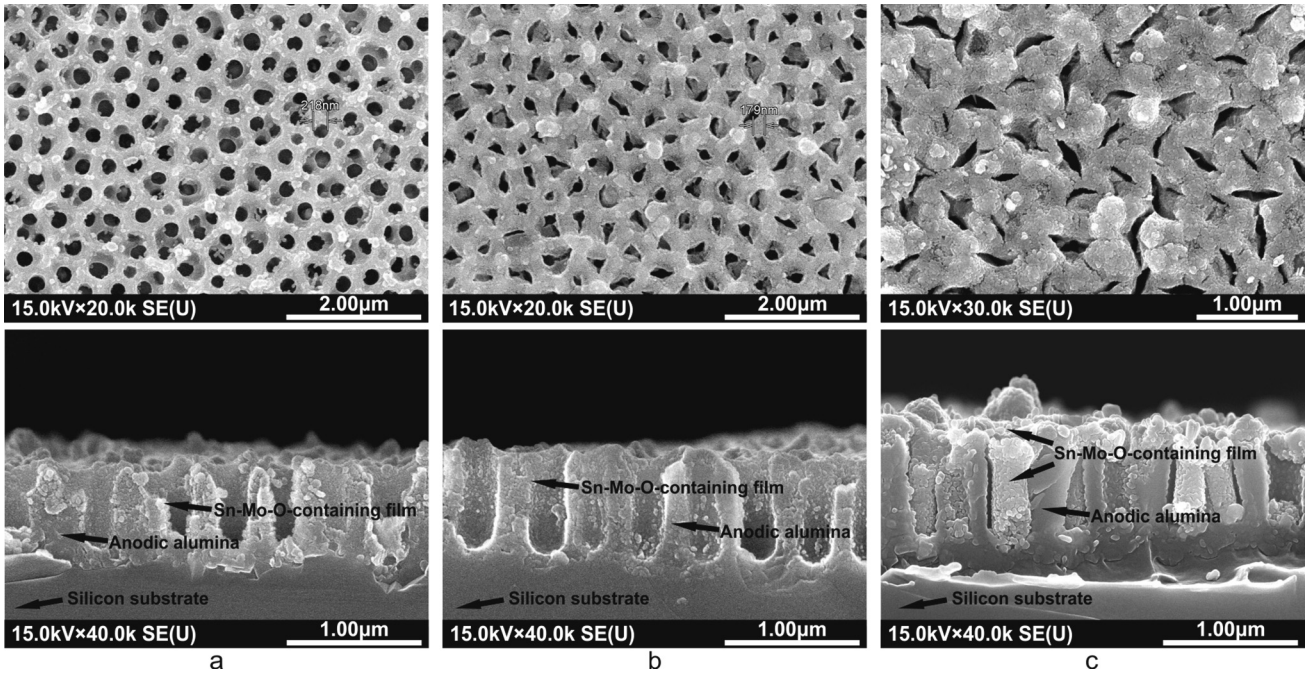

Fig. 3. SEM images of surfaces and cross-sections of Sn–Mo–O-containing films formed in AAMs after (a) 10, (b) 15 and (c) 20 SILAR cycles.

Table 1
Morphological parameters of Sn–Mo–O-containing films formed in AAMs.

Morphological parameters	AAM/ $(Sn\text{-}Mo\text{-}O)_{10}$	AAM/ $(Sn\text{-}Mo\text{-}O)_{15}$	AAM/ $(Sn\text{-}Mo\text{-}O)_{20}$
Number of SILAR cycles	10	15	20
Pores diameter on AAM surface, nm	216	128	80
Pores diameter on AAM cross-section, nm	228	210	pores are fully filled
Thickness of film on AAM surface, nm	111	125	139
Thickness of film in AAM pores, nm	12	21	pores are fully filled

matrix surface and probably led to decreasing in activation centers. With each subsequent cycle, the number of activation centers decreased, that led to a slowdown in film growth. Upon the detailed examination of SEM images of matrix cross sections, grains were detected in pores and on the surface structures, and grains size increases with increasing in the number of cycles. After 10 cycles, the grain size is 10–30 nm, and after 20 cycles, the grains grow to 100–120 nm. According to [28], films of SnO_2 compounds formed by the SILAR method are characterized by a high level of agglomeration with a small grain size on flat surfaces. Our results confirm this statement, and show that this degree of agglomeration is likely to increase on nanostructured surfaces.

The results of the electron-probe X-ray spectral microanalysis of Sn–Mo–O-containing film formed in AAM after 20 SILAR cycles are shown in Fig. 4. In the spectrum were detected elements correspond to the substrate (Si), the AAM (Al, O) and the synthesized film (Sn, Mo, O). Elemental analysis showed an atomic ratio of Sn/Mo = 1.29/2.72 at%. The atomic ratio was considered with according all elements containing in film.

3.2. Morphology and composition of Sn–Ni–Mo–O-containing films

The films of the composition Sn–Ni–Mo–O were deposited in AAM with thickness of 1000 nm and the pores diameters of 300 nm. Deposition was performed by the SILAR scheme; one Ni–Mo–O-monolayer was deposited after two Sn–Mo–O-monolayers. Total 21 layers were formed, included 14 Sn–Mo–O-layers and 7 Ni–Mo–O-layers. Morphology of the surface and the cross-section of Sn–Ni–Mo–O-containing film formed in the AAM are shown in Fig. 5.

The Sn–Ni–Mo–O-containing layer was deposited almost exclusively on the AAM surface, penetrating deep into the pores to an insignificant depth of only about 160 nm. As can be seen from the images, the total thickness of the deposited film was 1360 nm, and the surface coating on the matrix was about 1200 nm. As in the case of the Sn–Mo–O-containing layers, the film composition of Sn–Ni–Mo–O had a grain-like structure with grain sizes from 90 to 200 nm.

Fig. 6 shows the spectrum of the electron-probe X-ray spectral microanalysis of AAM with Sn–Ni–Mo–O-containing layer formed after 21 SILAR cycles. The spectrum contains responses corresponding to the substrate (Si), the AAM (Al, O) and the synthesized film (Sn, Ni, Mo, O). At that the atomic ratio of film components were Sn/Mo = 5.83/4.85 at% and Ni/Mo = 0.10/4.85 at%. So formed film consists of tin-molybdenum oxide doped with nickel. In comparison with Sn–Mo–O-containing film, atomic concentrations of tin and molybdenum in the Sn–Ni–Mo–O-film increased at 4.5 times for tin and at 1.8 times for molybdenum respectively. The low nickel concentration in the composition of the deposited film can be explained by the predominant activity of molybdenum cations during the co-precipitation of these two metals [28].

The investigations of the morphology and composition of Sn-Ni-Mo-O-containing films showed that the SILAR method allows the formation of metal oxide films consisting of 3 metal components. The continuous microstructure and deposition of the layer on the surface of the matrix can be explained by the insufficient activation of AAM pores before deposition.

3.3. Morphology and composition of Sn–Bi–Mo–O-containing films

The Sn–Bi–Mo–O-containing film was deposited in AAM with thickness of 1000 nm and pores diameters of 320 nm by the SILAR

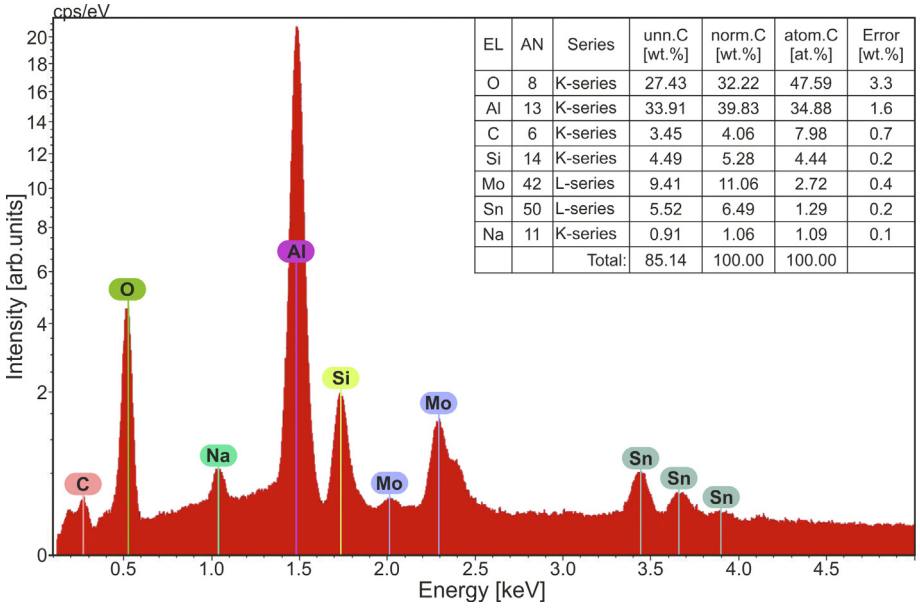

EL	AN	Series	unn.C [wt.%]	norm.C [wt.%]	atom.C [at.%]	Error [wt.%]
O	8	K-series	27.43	32.22	47.59	3.3
Al	13	K-series	33.91	39.83	34.88	1.6
C	6	K-series	3.45	4.06	7.98	0.7
Si	14	K-series	4.49	5.28	4.44	0.2
Mo	42	L-series	9.41	11.06	2.72	0.4
Sn	50	L-series	5.52	6.49	1.29	0.2
Na	11	K-series	0.91	1.06	1.09	0.1
		Total:	85.14	100.00	100.00	

Fig. 4. The the electron-probe X-ray spectral microanalysis of AAM with Sn–Mo–O-containing film formed after 20 SILAR cycles.

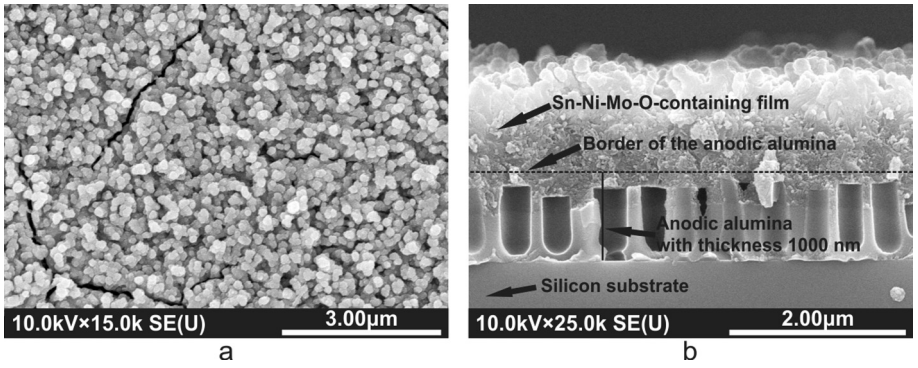

Fig. 5. SEM images of (a) surface and (b) cross-section of Sn–Ni–Mo–O-containing film formed in AAM after 21 SILAR cycles.

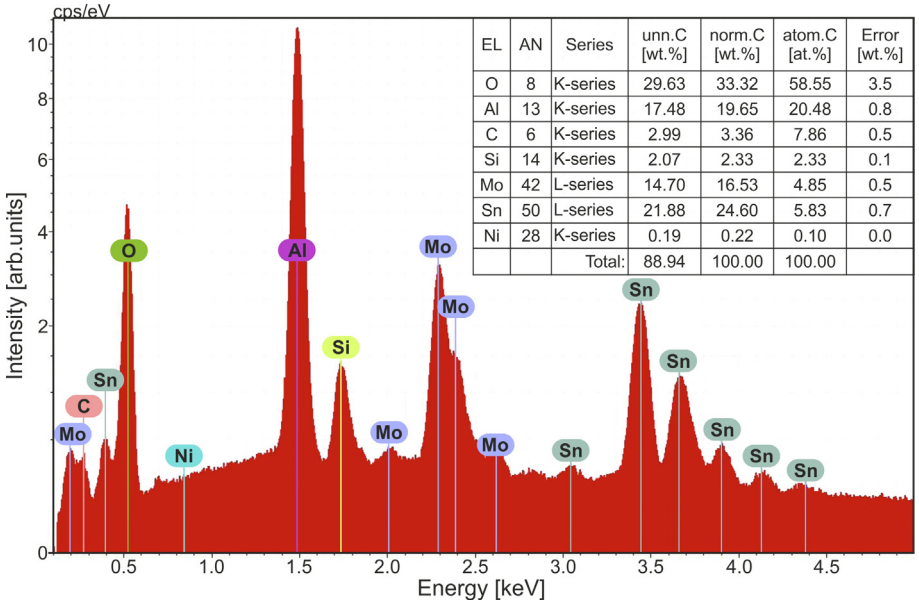

EL	AN	Series	unn.C [wt.%]	norm.C [wt.%]	atom.C [at.%]	Error [wt.%]
O	8	K-series	29.63	33.32	58.55	3.5
Al	13	K-series	17.48	19.65	20.48	0.8
C	6	K-series	2.99	3.36	7.86	0.5
Si	14	K-series	2.07	2.33	2.33	0.1
Mo	42	L-series	14.70	16.53	4.85	0.5
Sn	50	L-series	21.88	24.60	5.83	0.7
Ni	28	K-series	0.19	0.22	0.10	0.0
		Total:	88.94	100.00	100.00	

Fig. 6. The electron-probe X-ray spectral microanalysis of AAM with Sn-Ni-Mo-O-containing film formed after 21 SILAR cycles.

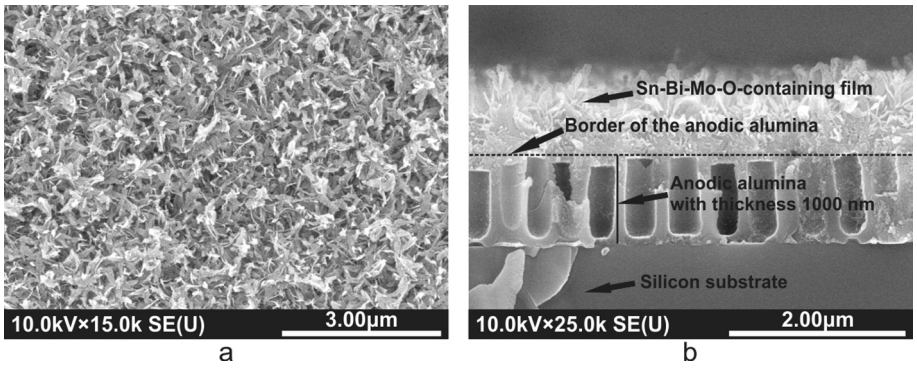

Fig. 7. SEM images of (a) surface and (b) cross-section of Sn–Bi–Mo–O-containing film formed in AAM after 20 SILAR cycles.

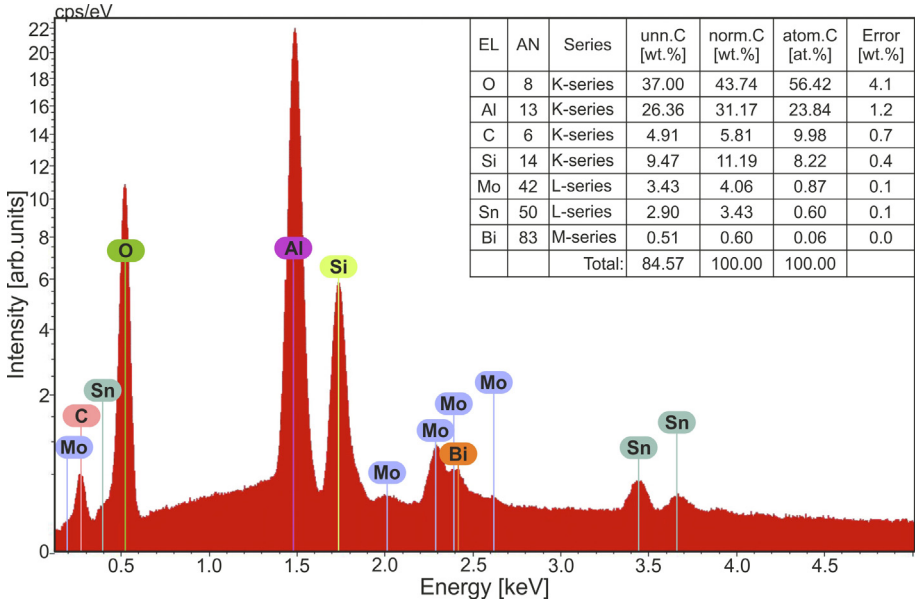

EL	AN	Series	unn.C [wt.%]	norm.C [wt.%]	atom.C [at.%]	Error [wt.%]
O	8	K-series	37.00	43.74	56.42	4.1
Al	13	K-series	26.36	31.17	23.84	1.2
C	6	K-series	4.91	5.81	9.98	0.7
Si	14	K-series	9.47	11.19	8.22	0.4
Mo	42	L-series	3.43	4.06	0.87	0.1
Sn	50	L-series	2.90	3.43	0.60	0.1
Bi	83	M-series	0.51	0.60	0.06	0.0
		Total:	84.57	100.00	100.00	

Fig. 8. The electron-probe X-ray spectral microanalysis of AAM with Sn-Bi-Mo-O-containing film formed after 20 SILAR cycles.

scheme. One Bi–Mo–O-containing layer was deposited after one Sn–Mo–O-containing layer; total were formed 20 layers included 10 Sn–Mo–O and 10 Bi–Mo–O-containing layers. Morphology of the surface and the cross-section of Sn–Bi–Mo–O-containing layer formed in the AAM are shown in Fig. 7. The metal oxide compound surface of the composition Sn–Bi–Mo–O, in contrast to the Sn–Ni–Mo–O-containing film having a granular morphology, is a flake-like structure.

The deposition of the Sn–Bi–Mo–O-containing layer was realized only on AAM surface, as in the case of Sn–Ni–Mo–O-film. The total thickness of the formed film was 1050 nm, the film thickness on the AAM surface was about 980 nm, penetrating deep into the pores to a depth of about 70 nm. Formed film has flake-like structure with flakes length of 300–500 nm.

The spectrum of the electron-probe X-ray spectral microanalysis of the metal oxide compounds Sn–Bi–Mo–O systems (Fig. 8) contains responses corresponding to the substrate (Si), the AAM (Al, O) and the synthesized film (Sn, Bi, Mo, O). However, the atomic ratios of the film components were quite differed with previous results – Sn/Mo = 0.60/0.87 at% and Bi/Mo = 0.06/0.87 at%. Also, formed film consists predominantly of tin-molybdenum oxide doped with bismuth. The atomic ratio of tin and molybdenum (Sn/Mo = 0.70) is almost two times less than the ratio in Sn–Ni–Mo–O-film (Sn/Mo = 1.20), but close to the ratio in Sn–Mo–O-film (Sn/Mo = 0.5). At that, Sn–Bi–Mo–O-containing film has the least concentration of the tin among formed films.

4. Conclusions

The multicomponent metal oxide compounds of the composition Sn–Mo–O, Sn–Ni–Mo–O, and Sn–Bi–Mo–O were formed in anodic alumina matrixes by the ionic layer deposition method. The electron microscopic studies showed that layers of different compositions cover AAM with varying degrees of pore filling, so the Sn–Mo–O-layers are uniformly distributed over the entire inner surface of the pores, and the Sn–Ni–Mo–O- and Sn–Bi–Mo–O-films predominantly precipitate on the AAM surface only partially penetrating deep into the pores. The investigations of the formed layers composition by the electron-probe X-ray spectral microanalysis showed that the ratio of tin to molybdenum in tin-molybdenum oxides changes dramatically after the introduction of nickel or bismuth into the compound.

Thus, using the SILAR method for the deposition of films in AAM allows forming structured multicomponent oxides consisted of two or three metal components. Formed multicomponent films have great potential to applicate in high-sensitivity gas sensors. The follow researches are forwarded to investigation of the anodic

alumina surface activation process and selection of deposition modes allow to fill the AAMs by three-component oxide compounds.

CRediT authorship contribution statement

Anna Zakhlebayeva: Conceptualization, Methodology, Investigation, Writing - original draft. **Andrei Lazavenka:** Conceptualization, Visualization. **Gennady Gorokh:** Supervision, Writing - review & editing.

Declaration of Competing Interest

The authors declare that they have no known competing financial interests or personal relationships that could have appeared to influence the work reported in this paper.

Acknowledgements

The Belarusian Republican Foundation for Fundamental Research supported this work by grant № F20RA-020, and the paper was prepared with funding from Mobility Scheme for Targeted People-to-People-Contacts (MOST, ID-code R-CVIG-52494).

References

[1] V.P. Tolstoy, S.D. Han, G. Korotcenkov, in: A. Umar, Y.-B. Hahn (Eds.), Metal Oxide Nanostructures and Their Applications, American Scientific Publishers, 2010, pp. 1–58.
[2] M. Nazir, M. Muhyuddin, F. Mughal, M.A. Basit, Proc. 16th Int. Bhurban Conf. Appl. Sci. Technol. (2019) 42–48.
[3] H.M. Pathan, C.D. Lokhande, Bull. Mater. Sci. 27 (2004) 85–111.
[4] G. Korotcenkov, V. Tolstoy, J. Schwank, Meas. Sci. Technol. 17 (2006) 1861–1869.
[5] G. Korotcenkov, L.B. Gulina, B.K. Cho, S.H. Han, V.P. Tolstoy, Mater. Chem. Phys. 128 (2011) 433–441.
[6] P.T. Babar, A.C. Lokhande, H.J. Shim, M.G. Gang, B.S. Pawar, S.M. Pawar, J.H. Kim, J. Colloid Interface Sci. 534 (2019) 350–356.
[7] A. Dey, Mater. Sci. Eng. B 229 (2018) 206–217.
[8] A. Ponzoni, C. Baratto, N. Cattabiani, M. Falasconi, V. Galstyan, E. Nunez-Carmona, F. Rigoni, V. Sberveglieri, G. Zambotti, D. Zappa, Sensors 17 (2017) 714 (27 pp).
[9] X. Liu, S. Cheng, H. Liu, S. Hu, D. Zhang, H. Ning, Sensors 12 (2012) 9635–9665.
[10] S. Yang, C. Jiang, S.-H. Wei, Appl. Phys. Rev. 4 (2017) 021304 (35 pp).
[11] Y. Deng (Ed.), Semiconducting Metal Oxides for Gas Sensing, Springer Singapore, Singapore, 2019.
[12] J. Liu, T. Wang, B. Wang, P. Sun, Q. Yang, X. Liang, H. Song, G. Lu, Sens. Act. B 245 (2017) 551–559.
[13] Z. Wang, Z. Li, J. Sun, H. Zhang, W. Wang, W. Zheng, C. Wang, J. Phys. Chem. C 114 (2010) 6100–6105.
[14] H. Tang, M. Yan, H. Zhang, S. Li, X. Ma, M. Wang, D. Yang, Sens. Act. B 114 (2006) 910–915.
[15] M. Punginsang, A. Wisitsoraat, A. Tuantranont, S. Phanichphant, C. Liewhiran, Mater. Sci. Semicon. Proc. 90 (2019) 263–275.
[16] J.W. Fergus, Sens. Act. B 123 (2007) 1169–1179.
[17] L.B. Gulina, V.P. Tolstoy, Thin Solid Films 440 (2003) 74–77.
[18] S.H. Chavan, B. Hou, A.T.A. Ahmed, Y. Jo, S. Cho, J. Kim, S.M. Pawar, S.N. Cha, A.I. Inamdar, H. Im, H. Kim, Sol. Energy Mater. Sol. Cells 185 (2018) 166–173.
[19] H. Masuda, K. Fukuda, Science 268 (1995) 1466–1468.
[20] H. Masuda, M. Satoh, Jpn. J. Appl. Phys. 35 (1996) L126–L129.
[21] F. Keller, M.S. Hunter, D.L. Robinson, J. Electrochem. Soc. 100 (1953) 411–419.
[22] J. Luoa, H. Zhenga, W. Chena, P. Zhenga, L. Zhenga, Q. Wub, Y. Zhanga, J. Magn. Magn. Mater. 489 (2019) 165449 (6 pp).
[23] A.A. Lozovenko, A.A. Poznyak, G.G. Gorokh, J. Phys. Conf. Ser. 1124 (2018) 022013 (7 pp).
[24] G.G. Gorokh, M.I. Pashechko, J.T. Borc, A.A. Lozovenko, I.A. Kashko, A.I. Latos, Appl. Surf. Sci. 43 (2018) 829–835.
[25] A. Pligovka, A. Zakhlebayeva, A. Lazavenka, J. Phys. Conf. Ser. 987 (2018) 012006 (5 pp).
[26] G.G. Gorokh, A.I. Zakhlebayeva, A.I. Metla, V.V. Zhilinskiy, A.N. Murashkevich, N.V. Bogomazova, J. Phys. Conf. Ser. 917 (2017) 092011 (6 pp).
[27] W. Lee, S.-J. Park, Chem. Rev. 114 (2014) 7487–7556.
[28] G. Korotcenkov, S.D. Han, B. Cho, V. Tolstoy, Process. Appl. Ceram. 3 (2009) 19–28.